A Climatic Based Asymmetric Mapping Function Using a Dual Radiosonde Raytracing Approach

Reza Ghoddousi-Fard and Peter Dare
Geodetic Research Laboratory, Department of Geodesy and Geomatics Engineering
University of New Brunswick

BIOGRAPHY

Reza Ghoddousi-Fard is a Ph.D. student at the University of New Brunswick (UNB). He obtained a B.Sc.E. in Geomatics and a M.Sc.E. in Geodesy in 1995 and 1999 respectively from K.N.Toosi University of Technology, Tehran, Iran. He has been involved in Geomatics projects, research and teaching since 1995. His current research focus is on GPS meteorology and neutral atmospheric modeling.

Peter Dare is the Chair of the Department of Geodesy and Geomatics Engineering at UNB. He obtained a B.Sc. (Hons) in Land Surveying Sciences from North East London Polytechnic in 1980, an M.A.Sc. in Civil Engineering from the University of Toronto in 1983 and a Ph.D. in Geodesy from the University of East London in 1996. He joined UNB in 2000 and became the Chair of the Department in 2002.

ABSTRACT

The delay induced by the neutral part of the atmosphere on GPS signals still remains one of the most important accuracy limiting factors in high precision positioning applications. Estimation of the residual neutral atmospheric delay (after considering an a priori model) is common practice. It is widely accepted to model the neutral atmospheric delay in the zenith direction and multiply the zenith values by a known mapping function. During the last few decades a large number of mapping functions have been developed. Most of these mapping functions are based on a symmetric atmosphere assumption. This assumption seems to be unrealistic especially when dealing with GPS signals received from low elevation angle satellites. Low elevation signals first reach the neutral atmosphere with a horizontal distance of hundreds of kilometres from the location of the receiver, where the atmospheric condition is likely to be different than at the location of the GPS receiver. Furthermore, a small change in azimuth for a low elevation satellite creates a much larger change in the location of where the GPS signal enters the neutral atmosphere compared to the same change in azimuth from a high elevation satellite.

Previous studies suggested the effect of azimuthal variations in the atmosphere should be considered in high precision GPS positioning applications. The effect of azimuthal variations on high accuracy positioning and zenith delay estimation might be crucial where the use of low elevation data is important and the amount of the wet delay is smaller than other regions (hence, more accurate estimation of the delay is required to achieve the same relative accuracy); both might be the case in high latitudes.

In this paper a new mapping function has been developed based on a semi-3D raytracing of radiosonde data spanning one year in Canada and the northern US. All radiosondes in a fixed radius around each one of the radiosondes in the mentioned region were considered to perform dual raytracing (i.e., using two radiosondes launched at the same time). The result of this semi-3D raytracing which has dependency on azimuth (resulting from each pair of radiosondes) was compared with the raytracing results from the one central radiosonde (normal raytracing with azimuthal symmetric assumption). The differenced values over one year of data contain variations of slant delays as a function of azimuth and location. A statistical approach was employed to model these variations by means of fitting functions to the data series resulting from different low elevation angles. The primary results show a clear systematic slant hydrostatic delay difference in the North-South direction over all months whereas no such clear trend can be seen in East-West direction. This is in agreement with other studies using low resolution numerical weather models. Due to a lower effective height of the atmosphere impacting on the wet delay, and sparcity of the radiosonde stations, this approach might not be suitable for studying asymmetry in

the wet delay. However, due to the fact that the hydrostatic part of the delay is about 10 orders of magnitude larger than the wet part, a more accurate hydrostatic mapping function is of more concern than a wet one.

Further research to validate GPS tropospheric gradient estimation using the dual raytracing approach at collocated GPS and radiosonde stations is ongoing. The effect of the new mapping function on positioning and zenith delay estimation might be seen in the results of long term processing of GPS data.

INTRODUCTION

Neutral atmospheric delay in radiometric space techniques including GNSS has been a main accuracy limiting factor. The common practice in GNSS analysis is to use an a priori model for the zenith direction and relate the zenith values to any direction using a known mapping function. A large number of mapping functions have been developed in the past decades. Most of these are based on the assumption of a symmetric atmosphere around the site. Clearly, this assumption might not be reasonable in case of local weather anomalies. Furthermore, even with nominal weather conditions, the assumption will be violated when low elevation angle GNSS signals are used. The use of data from low elevation satellites is essential to decorrelate the height component and zenith delay estimations.

Although estimation of residual neutral atmospheric delay is a common approach in GNSS analysis, the impact of an a priori model on the estimated coordinate and zenith neutral atmospheric delays could be significant in some applications (see e.g. Tregoing and Herring [2006]). Similarly, systematic errors existing in the mapping function may result in systematic errors in estimated parameters. This may be of concern in some applications such as studying the variation of zenith wet delays for climate research. This can be crucial in dry regions where there is a small amount of wet delay and hence more accurate estimation is required to reach the same relative accuracy or when high accuracy coordinates are required for geodynamic studies.

In this paper the use of radiosondes for modelling large scale gradients in the neutral atmosphere is investigated. A one year dataset of radiosondes available in Canada and northern US is employed to provide a database of elevation angle as well as azimuthally dependent values using a semi 3D raytracing approach. A hydrostatic gradient model for the investigated region is then retrieved using a statistical approach.

BACKGROUND

Similar to the common approach to deal with the symmetric part of the delay, the use of an elevation dependent function to map the horizontal azimuthally dependent delays has also been used to model the asymmetric part.

The geodetic azimuth (α) and elevation angle (ε) between two points (with geometric distance S) can be related to local geodetic coordinate system as follows:

$$N = S.\cos\varepsilon.\cos\alpha$$

$$E = S.\cos\varepsilon.\sin\alpha \qquad (1)$$

$$h = S.\sin\varepsilon$$

where N, E and h are north, east and height components respectively. From (1) the position vector of a point on the path can be written as follows:

$$\vec{x}(\varepsilon,\alpha) \cong h.\cot\varepsilon.(\cos\alpha.\hat{n} + \sin\alpha.\hat{e}) \qquad (2)$$

where $\hat{n}$ and $\hat{e}$ are the unit vectors in the north and east respectively.

Based on the above relations, Davis et al. [1993] (with the assumption of linear variation of refractivity with horizontal distance) defined a gradient mapping function as follows:

$$m_{asym}(\varepsilon,\alpha) = m_{sym}(\varepsilon).\cot\varepsilon'.$$
$$(G_N.\cos\alpha + G_E.\sin\alpha) \qquad (3)$$

where $m_{sym}(\varepsilon)$ is a symmetric mapping function (i.e. not a function of azimuth), ε' is the refracted elevation angle, and G_N and G_E are the delay gradients in the north and east directions respectively. Using an approximate relation between the refracted and unrefracted (vacuum) elevation angle given by Bean and Dutton [1966], the Davis gradient mapping function in (3) is given as:

$$m_{asym}(\varepsilon,\alpha) \cong m_{sym}(\varepsilon).\cot\varepsilon.$$
$$(1 - 10^{-6}N_s\csc^2\varepsilon).(G_N.\cos\alpha + G_E.\sin\alpha) \qquad (4)$$

where N_s is the total surface refractivity.

Later, MacMillan [1995] and MacMillan and Ma [1997] applied the gradient model of Davis (by replacing ε' simply by ε in equation 3) in VLBI analysis and noted that the results are not sensitive to whether $m_{sym}(\varepsilon)$ is replaced by a dry or a wet mapping function. Chen and Herring [1997] replaced the $m_{sym}(\varepsilon).\cot\varepsilon'$ term in

equation (3) with an asymmetric mapping function as follows:

$$m_{asym}(\varepsilon) = \frac{1}{\sin\varepsilon.\tan\varepsilon + C} \qquad (5)$$

where they found the value of C to be 0.0031 and 0.0007 for the hydrostatic and non hydrostatic parts respectively. However, they used a combined value of 0.0032 in their VLBI analysis as it is difficult to estimate the hydrostatic and non hydrostatic parts separately.

Figure 1 shows the Davis gradient mapping function with hydrostatic Niell mapping function [Davis(NMFh)], Davis gradient mapping function with non-hydrostatic Niell mapping function [Davis (NMFnh)],Chen and Herring hydrostatic mapping function [CH(H)] and Chen and Herring non-hydrostatic mapping function [CH(NH)] values over low elevation angles. It can be seen that the mapping functions differ significantly in low elevation angles. For example, the difference between Davis with hydrostatic Niell mapping function (hereafter refer to as Davis) and hydrostatic mapping function of Chen & Herring (hereafter refer to as CH) is about 34 mm for a ray at 5 degree elevation angle assuming a horizontal gradient delay of 1.5 mm.
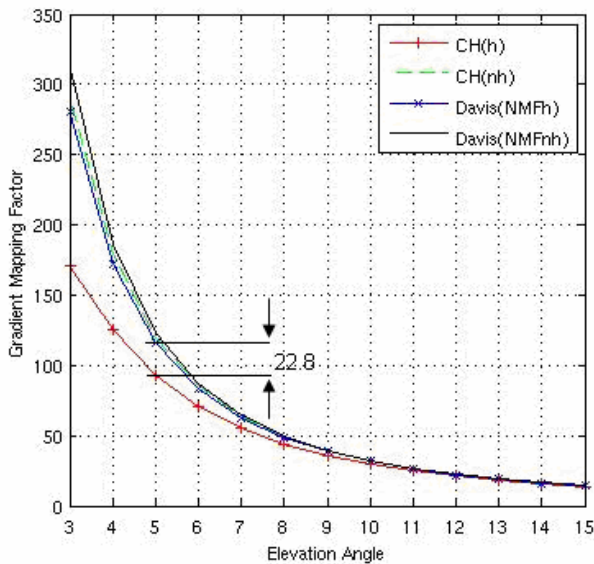

Figure 1- Gradient mapping functions comparison over low elevation angles

There have been some efforts to have more realistic a priori values for the asymmetric part of the neutral atmospheric delay. Ifadis and Savvaidis [2001] used 5 radiosondes to study the horizontal variations of the atmosphere. However, they were unable to model the delay variation in their case study. More recently the use of Numerical Weather Prediction (NWP) models for the development of an asymmetric mapping function have been investigated (see e.g. Niell [2001] and Beoehm and Schuh [2005]). However, the proposed approaches require

access and manipulation of NWP data together with a number of assumptions for simplification of the process.

SEMI 3D RAYTRACING

Ray tracing has been a common approach to deal with radio signal propagation through the atmosphere for a long time (see e.g. Bean & Dutton [1966]). Assuming a symmetric atmosphere around the point of interest, the layers which are required for numerical integration are made through vertical profiles of measurements. Hence the results have no dependency on azimuth. An alternative could be using a 3D or semi 3D atmospheric field. The former might be possible with a NWP model. However, for regional statistical studies, one may also benefit from rather spatially irregularly distributed radiosondes.

The neutral atmosphere contributes to the hydrostatic part of the delay up to an altitude of about 70-80 km. Figure 2 shows the effect of reducing the top level of integration in the zenith and 5 degree elevation slant delay. From the figure one can conclude that ignoring the atmosphere above 60 km may result in a few mm slant delay error and more than 0.5 mm in the zenith delay.
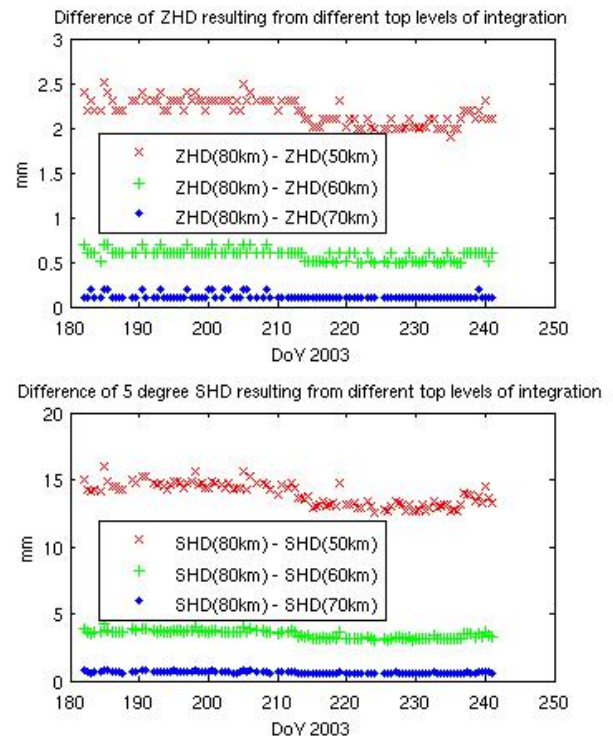

Figure 2- Change of zenith and slant hydrostatic delay when top of the integration is 50, 60 and 70 km rather than 80km. RAOB: Churchill

Figure 3 shows the horizontal distance of the station from the point where the signal reaches the top of the neutral

atmosphere. One can see that for example a ray with 3 degree apparent elevation angle first reaches the top of the neutral atmosphere (height of 80 km) at a horizontal distance of about 733 km from a station at mid latitude. At a high latitude station, GPS constellation allows observations at azimuths of both 0 and 180 degree at e.g. 3 degree elevation angle. This means two rays might reach the top of the neutral atmosphere with a horizontal separation of about 1460 km from each other where the atmospheric condition (including the thickness of the atmosphere which affect the hydrostatic component) is likely to be different.
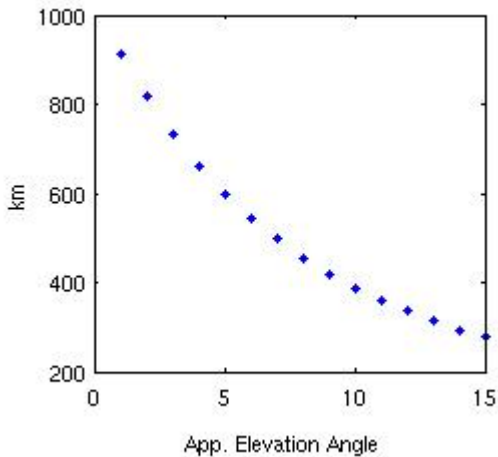

Figure 3- Horizontal distance of the slant path from the station at the top of the neutral atmosphere (80 km altitude)

Large scale azimuthal variation of the atmosphere around a site may be investigated using radiosonde observation profiles. Each radiosonde can be considered as a center of neighborhood with a constant radius. All other radiosondes located in this neighborhood could contain azimuthal atmospheric information in the direction made by the central and each adjacent radiosonde. Hence, each neighborhood could contain directional information that could be useful for asymmetric studies in a statistical sense.

In this research, two meteorological profiles (resulting from two radiosondes launched at the same time) were used to retrieve more realistic parameters along the ray path. Figure 4 shows a schematic ray path from GPS satellite to location of "receiver" (in this case a radiosonde launch site labeled as r_1). Meteorological values of the neighborhood radiosonde are first interpolated vertically to the same vertical levels of the central radiosonde. We refer to Ghoddousi-Fard [2006] for more details on vertical interpolation of radiosonde profiles and single radiosonde raytracing. For online access to raytracing results at a user location using radiosondes, global and regional Canadian NWP models, we refer to UNB's Online Raytracing (Ghoddousi-Fard

[2007]). The meteorological parameters for refractivity calculations at each integration step on the path (e.g. point p in Figure 4) were derived by linear interpolation between two radiosondes (r_1 and r_2) using equation 6, where l_1 and l_2 are meteorological parameters from first and second radiosondes respectively, R is the radius of the earth and φ_p and ϕ_P are the central angles (see Figure 4). In case a ray passes the second radiosonde, only the values from the second radiosonde was used for refractivity calculations.

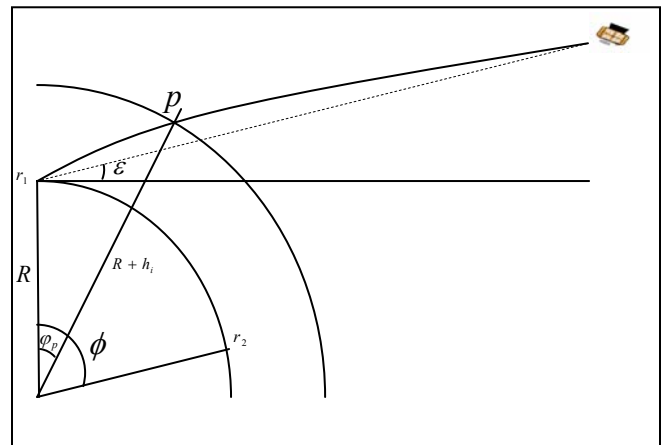$$l_p = l_1 + (l_2 - l_1) \times \frac{R\varphi_p}{R\phi} \tag{6}$$

Figure 4- A schematic representation of raytracing

A software package has been developed to perform raytracing using both single and dual raytracing. The software finds all radiosondes in a radius of 1000 km around each one of the radiosondes. The difference between the slant delay from both dual and single radiosonde raytracing approaches contains information about the contribution of the atmosphere in the asymmetric part of the delay in the direction of the two radiosondes.

REGIONAL STUDY OF GRADIENTS

Using 71 available radiosondes in the investigated area (see Figure 5) in year 2004, 555 radiosonde pairs were made. This resulted in 326515 slant delays per elevation angle over the whole year. For all raytraced elevation angles (1-12 and 15 degrees) this made 4,244,695 slant delays for both single and dual raytracing approaches. This large database was then employed for statistical analysis.
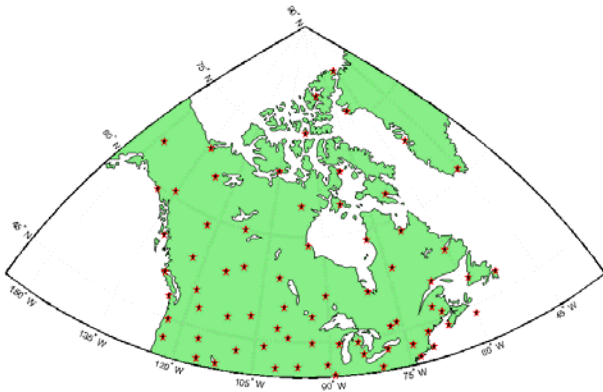
Figure 5- Location of radiosondes in the investigated area

Figure 6 shows the average of the difference between dual and single radiosonde raytracing at a 3 degree apparent elevation angle for the slant hydrostatic delay. The error bars are the standard deviation over the whole of 2004. It can be seen that all possible pairs of radiosondes provide almost a full range of azimuths. The black curve in the figure (in the polar plots as well) is the result of a nonlinear least square fit of a trigonometric function which will be discussed in the next section of the paper.
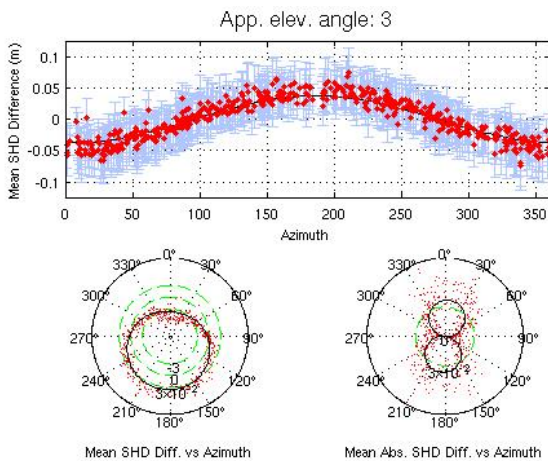

Figure 6- Upper plot: Average differences of dual – single raytracing of slant hydrostatic delay vs. azimuth (red dots with error bars) and fitted model (black curve). Lower plot left: Same as above but in polar plot and without error bars. Lower plot right: Same as above but for absolute differences.

The lower left polar plot of Figure 6 shows a systematic decrease of SHD toward north (zero azimuths) and an increases towards south. The plot in lower right of Figure 6 shows values around zero in east west direction.

The variation of yearly averaged values vs. latitude and azimuth can be seen in the 3D plot in Figure 7. A clear systematic north south average gradient can be seen in Figures 6 and 7. The results for slant wet delay do not

show such a clear trend. This might be due to the limitation of the current approach in which the closest radiosonde pairs in the investigated area are about 115 km from each other. Hence the current semi 3D raytracing approach cannot detect the usually smallscale variation in the wet delay behavior. However, even with this approach, a slight north south wet gradient can be detected in some months (not shown here). The north south gradient for both hydrostatic and wet components of the delay is expected. The former is mainly the result of decreasing the thickness of the atmosphere toward the pole and the later is due to the general decrease of humidity with increasing latitude in the investigated area. One can see as an example the thickness map of the atmosphere (500 hpa -1000 hpa isobaric levels) and ZWD map over Canada and northern US for an arbitrary epoch in Figures 8 and 9 respectively. The values used to produce the maps are calculated using the Canadian high resolution regional NWP model.
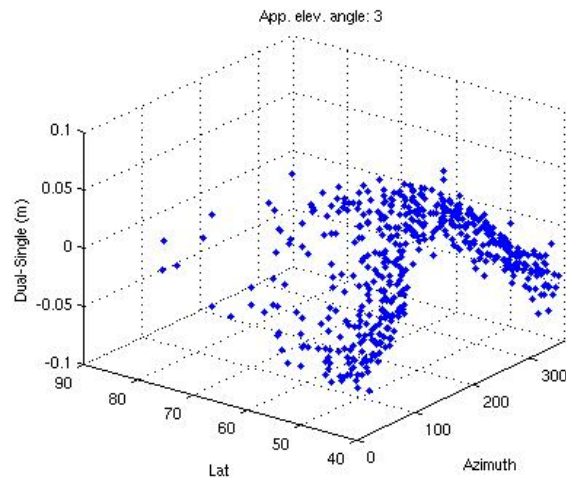

Figure 7- Yearly average differences of dual – single raytracing of slant hydrostatic delay vs. azimuth and latitude.
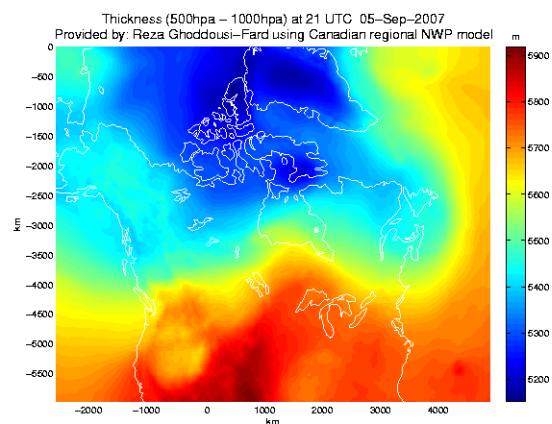

Figure 8- Thickness of the atmosphere at 21 UTC 05-Sep-2007 over area covered by regional Canadian NWP model
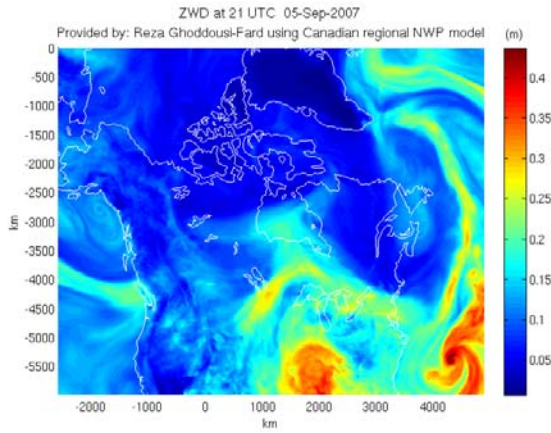
2874

Figure 9- ZWD at 21 UTC 05-Sep-2007 over area covered by regional Canadian NWP model

MODELLING THE HYDROSTATIC GRADIENTS

Using the created database, an effort was made to model the nominal hydrostatic gradients in the investigated area. In order to study the monthly variation of the hydrostatic delay the database is decimated into 12 monthly periods.

The following function was fitted to the differenced values (dual – single raytracing slant hydrostatic results) using a nonlinear weighted least squares approach:

$$d = g_N . \cos(az) + g_E \sin(az) \qquad (6)$$

where d is the azimuth dependent monthly averaged differenced values, az is the azimuth and g_N and g_E are being estimated. The weights were derived from the inverse of the variance of the monthly values. The values beyond $\pm 3\sigma$ were ignored. Compared to equation (3), one can see that the estimated values in equation (6) contain the delay gradients as well as the elevation dependent part. The procedure was carried out for all 12 months. The estimated parameters are plotted in Figure 10. The north south elevation dependent gradients become significant at low elevation angles. There is also a yearly average change up to more than 4 cm in this component with the largest values in the winter months. As expected, the east west component has a smaller average value and it is hard to interpret (lower plot in Figure 10). One can also see in Figure 10 the north-south and east-west gradients result from a whole year.

To model the estimated gradients, the following exponential functions were fitted to the gradients:

$$\hat{g}_N = a_N . e^{b_N . \varepsilon} \qquad (7)$$

$$\hat{g}_E = a_E . e^{b_E . \varepsilon} \qquad (8)$$

where $\hat{g}_N$ and $\hat{g}_E$ are the elevation dependent gradients, a_N, b_N, a_E and b_E are given in Table 1 and ε is the elevation angle.

COMPARISON OF DIFFERENT MAPPING FUNCTION RESULTS

In order to validate the result of the derived model in the previous section with an independent data set, the dual raytracing approach over the same region was repeated but using one month of data in 2007. Comparison with the mapping functions represented in equations 3 and 5 is not directly possible as the horizontal gradient delays (G_n and G_e) must be estimated (or retrieved) first. The horizontal gradient delays may be retrieved from a NWP model. We employed a numerical gradient calculation algorithm which uses up to 16 nearest profiles from a global high resolution Canadian NWP model. Our gradient calculation approach is different than the 3 vertical profile approach used by Boehm and Schuh [2007]. They calculate the gradients using the model of the European Centre for Medium-range Weather Forecasts for VLBI analysis. A detailed explanation of our approach to retrieve the horizontal delay gradients from the Canadian NWP model is beyond the scope of this paper.

Gradient calculation using NWP was performed at some locations collocated with the investigated radiosondes, including the central radiosonde shown in Figure 11 (The Pas, MB). The comparison between Davis mapping function, CH mapping function (both functions using NWP retrieved hydrostatic horizontal delay gradients), the dual raytracing approach and the result of the fit to the 2004 data (equations 7 and 8) are plotted in Figure 12 for each azimuth made between radiosonde pairs at a 3 degree elevation angle over the month of August 2007.

In Figure 13, a comparison with dual RAOB raytracing approach at each of the directions, then summarized as error bar plots (mean and standard deviation), is shown. One can see that in this investigated case the CH mapping function, followed by the average fit from 2004 data (this paper), provided closer results to the dual RAOB raytracing approach than the Davis mapping function. One should note that in both CH and Davis mapping functions NWP horizontal delay gradients were used while the elevation angle dependent part is absorbed in the fit to the 2004 data (equations 7 and 8).

The difference between Davis and CH is only on the elevation dependent part. We replaced $m_{sym}(\varepsilon)$ in equation 3 with hydrostatic Neill mapping function in order to use the Davis mapping function. Due to a larger

elevation dependent part, the Davis mapping function provides larger values than CH mapping function. The same NWP horizontal delay gradients are used in both Davis and CH mapping functions.
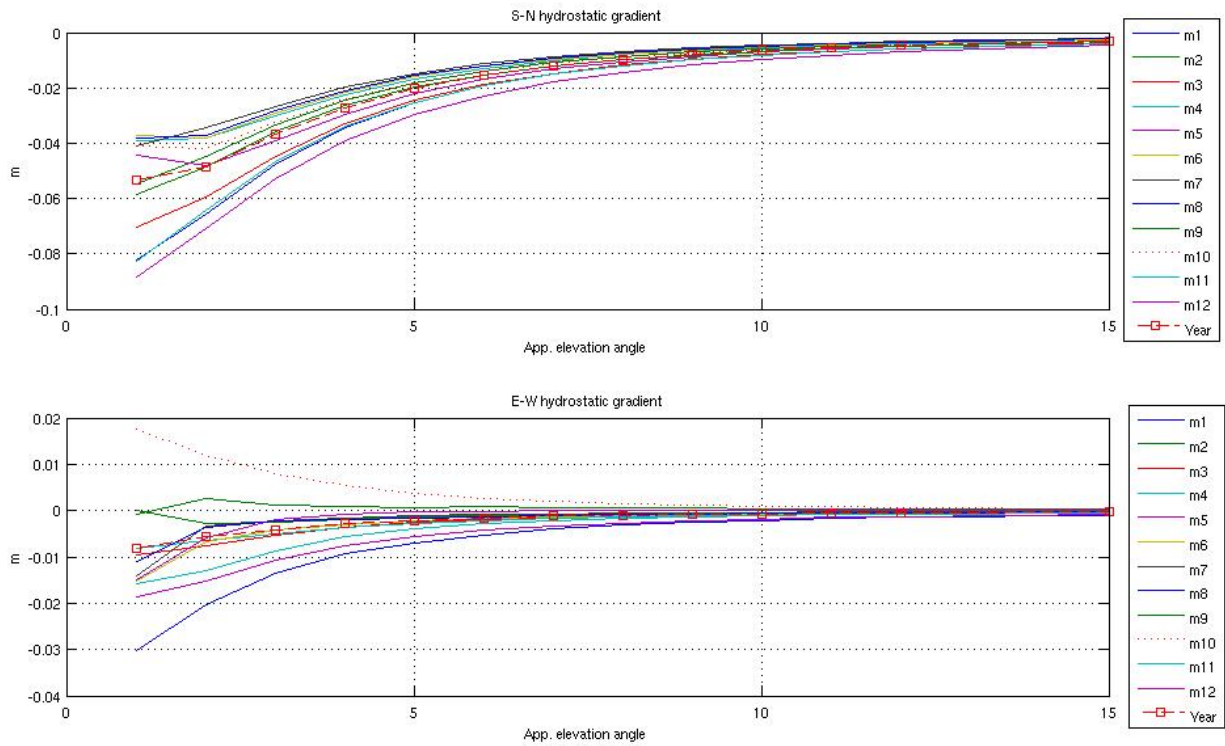

Figure 10- The estimated elevation dependent hydrostatic gradients at low elevation angles for each month and the whole year of 2004.

Table 1- Estimated parameters of exponential fit to north south (index N) and east west (index E) components together with rms of the fits. Unit: metre

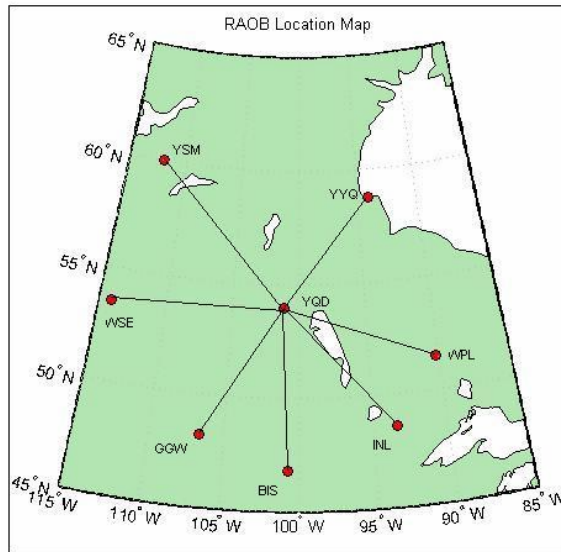| Month	a_N	b_N	rms_N	a_E	b_E	rms_E
1	-0.1095	-0.2785	0.0015	-0.0419	-0.3554	0.0007
2	-0.0727	-0.2656	0.001	-0.001	-0.0312	0.0008
3	-0.0936	-0.2546	0.0015	-0.0133	-0.3149	0.0002
4	-0.0534	-0.223	0.0018	-0.0107	-0.258	0.0001
5	-0.063	-0.2045	0.0031	-0.0391	-0.9605	0.0001
6	-0.0519	-0.2241	0.0021	-0.0251	-0.5588	0.0007
7	-0.0542	-0.2503	0.0008	-0.0426	-1.1287	0.0007
8	-0.0524	-0.2317	0.0017	-0.0217	-0.7336	0.0008
9	-0.0772	-0.2571	0.0012	0.0006	-0.0198	0.0007
10	-0.0567	-0.2174	0.0022	0.0251	-0.3718	0.0003
11	-0.1096	-0.2814	0.0014	-0.0227	-0.3247	0.0005
12	-0.1157	-0.2614	0.0014	-0.025	-0.2806	0.0004
Year	-0.0721	-0.2416	0.0018	-0.0112	-0.3224	0.0002

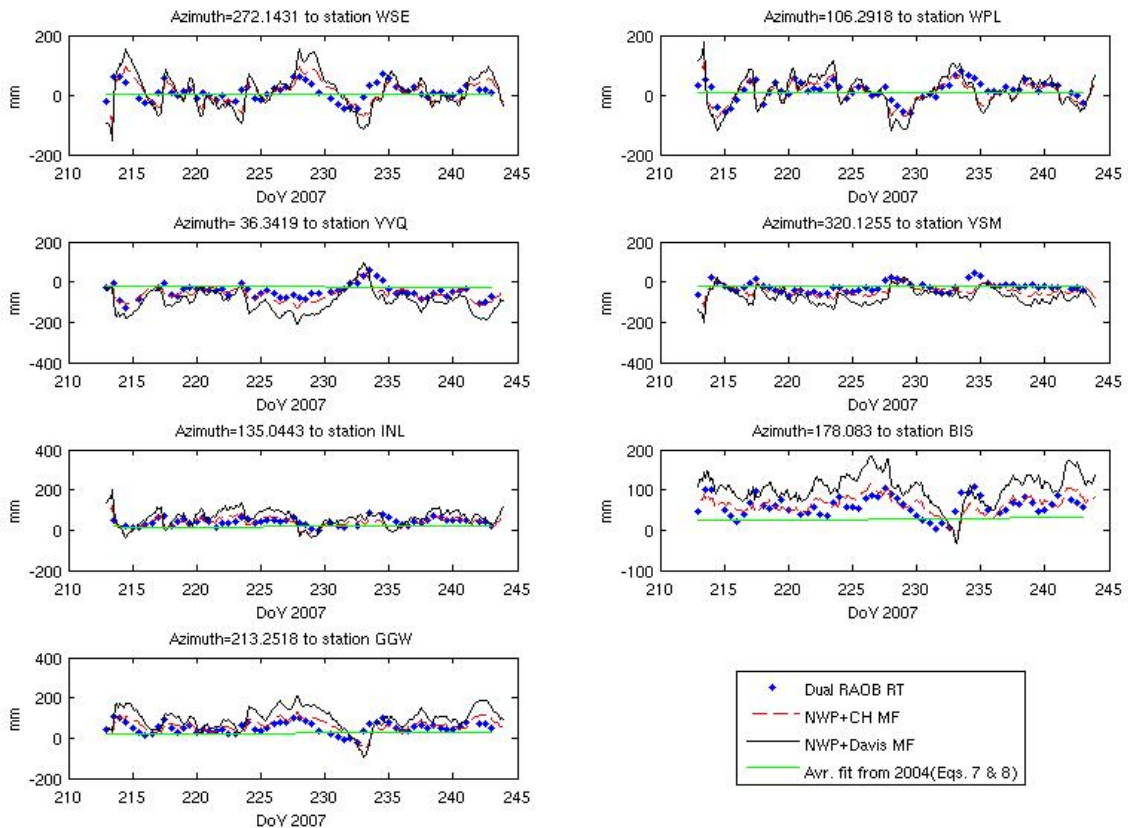**Figure 11- Location of radiosondes used for validation**

Figure 12 – Comparison between Davis asymmetric mapping function, Chen & Herring asymmetric mapping function (both with NWP retrieved horizontal delay gradients), dual RAOB raytracing approach and the fit to the 2004 data (equations 7 and 8) at central station YQD (The Pas, MB). Elevation angle: 3°.
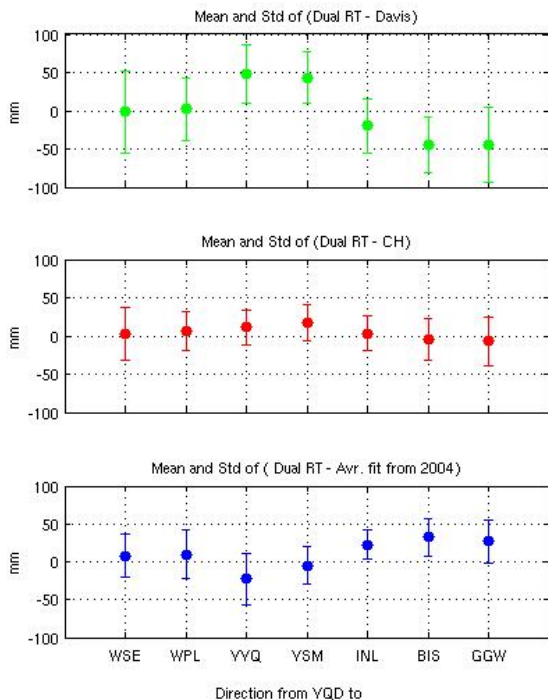
Figure 13- Mean and standard deviation of Dual RAOB raytracing – Davis (Upper plot), Dual RAOB raytracing – Chen & Herring (middle plot) and Dual RAOB raytracing – average fit from 2004 (lower plot) for each direction shown in Figure 9 with 3 degree elevation angle

CONCLUSION AND OUTLOOK

In this paper we have investigated the possibility of using radiosondes to study the asymmetric part of the neutral atmospheric delay. It has been shown that this approach can detect the average hydrostatic gradients behavior in a statistical sense. Due to sparcity of radiosonde stations at some locations (e.g. high latitudes) we did not derive a fit that was location dependent. The derived functions may be seen as an average value over the whole investigated area. As can be seen in Figure 12, the hydrostatic delay variation in azimuth may reach to about 150 mm for a ray at 3 degree elevation angle. Although all mapping functions and approaches that have been employed are affected by several assumptions, inter comparison among rather independent approaches show a general agreement among them. However, the uncertainty in all investigated approaches still seems high compared to the amount of the asymmetric delay itself. The results of this statistical analysis in the investigated area quantify a clear average north south gradient which can have a systematic effect on GNSS high accuracy analysis. This might be of more concern in the arctic where the low elevation angle observations in all azimuths (including the north direction

unlike mid latitudes) may be used due to the GPS constellation.

Investigating the effect of a priori gradient models in GPS analysis is challenging. However, as the hydrostatic gradient has a systematic behavior in north south direction, this might affect the GPS estimated parameters (including neutral atmospheric delay estimates). Further research includes studying the systematic effect of gradient on long term GPS coordinate and zenith wet delay estimation. Use of longer radiosonde data set and other data sources might provide a better average fit for the study shown here.

ACKNOWLEDGEMENT

REFERENCES

Bean, B.R. and E.J. Dutton (1966). *Radio Meteorology*. National Bureau of Standards Monograph 92, U.S. Government Printing Office, Washington, D.C.

Boehm J., Ess M. and Schuh H. (2005), Asymetric Mapping Functions for CONT02 from ECMWF. In M.Vennebusch and A.Nothnagel (Eds.): Proceedings of the 17th Working Meeting on European VLBI for Geodesy and Astrometry. April 22-23, pp. 64-68.

Boehm J. and H. Schuh (2007), "Troposphere gradients from the ECMWF in VLBI analysis." *Journal of Geodesy*, 81:403-408 DOI 10.1007/S00190-007-0144-2

Chen G. and Herring T. A. (1997), " Effects of atmospheric azimuthal asymmetry on the analysis of space geodetic data." *Journal of Geophysical Reseach*, Vol. 102, No. B9. pp 20489-20502

Davis, J.L., G. Elgered, A.E. Niell, and C.E. Kuehn (1993). "Ground-based measurement of gradients in the "wet" radio refractivity of air." *Radio Science*, Vol. 28, No. 6, pp. 1003-1018.

Ghoddousi-Fard R. (2007), Online Raytracing, Department of Geodesy and Geomatics Engineering, University of New Brunswick [Online] 1 April 2007 http://galileo.gge.unb.ca/main.shtml

Ghoddousi-Fard R. (2006). "Comparison of IGS and Radiosonde Determination of ZTD in the Canadian Arctic." Proceedings of ION GNSS 2006, 19th

International Technical Meeting of the Satellite Division of The Institute of Navigation, Fort Worth, Texas, Sept. 26-29, 2006, pp. 1936-1944

Ifadis, I.M. and P. Savvaidis (2001). "Space to Earth Observations: Approaching the Atmospheric Effect." *Phys. Chem. Earth (A)*, Vol. 26, No. 3, pp. 195-200.

MacMillan, D.S. (1995). "Atmospheric gradients from very long baseline interferometry observations." *Geophysical Research Letters*, Vol. 95, No. 9, pp. 1041-1044.

MacMillan, D.S. and C. Ma (1997). "Atmospheric gradients and the VLBI terrestrial and celestial reference frames." *Geophysical Research Letters*, Vol. 24, No. 4, pp. 453-456.

Niell A.E. (2001), An a priori Hydrostatic Gradient Model for Atmospheric Delay. In: D. Behrend and A Rius (Eds.): Proceedings of the 15th Working Meeting on European VLBI for Geodesy and Astrometry, Institut d'Estudis Espacials de Catalunya, Consejo Superior de Invetigaciones Cientificas, Barcelona, Spain, 2001

Tregoning P. and T.A. Herring (2006). " Impact of a priori zenith hydrostatic delay errors on GPS estimates of station heights and zenith total delay. *Geophysical Research Letters*, Vol. 33, L23303, DOI:10.1029/2006GL027706